

# TEMPORAL AND SPATIAL VARIATIONS IN THE PLANETARY-SCALE OUTGOING LONG-WAVE RADIATION AS DERIVED FROM TIROS II MEASUREMENTS

JAY S. WINSTON and P. KRISHNA RAO

Meteorological Satellite Laboratory, U.S. Weather Bureau, Washington, D.C.

[Manuscript received July 22, 1963; revised September 18, 1963]

## ABSTRACT

Daily composite charts of outgoing long-wave radiation between latitudes 55°N. and 55°S. were derived from TIROS II measurements for 26 days between late November 1960 and early January 1961. Samples of these charts reveal the wealth of information available about the radiation patterns over the earth and about the synoptic distributions of the major cloud fields. Mean maps of outgoing long-wave radiation for four periods of generally more abundant radiation data portray the broad-scale variations in the radiation pattern both geographically and in time. For the Northern Hemisphere these maps show how the long-wave radiation varied during some very large-scale changes in 700-mb. mean flow which were part of a remarkable energy, or index, cycle in this period. Most pronounced were the sharp decreases in outgoing radiation that accompanied the penetration of westerlies into the subtropics where anticyclones had prevailed previously. In the Southern Hemisphere some sizable temporal variations also occurred; these appeared to be representative of a change in circulation from a zonal to a more meridional type. Average latitudinal profiles of the outgoing radiation for these four mean periods and for the entire 26 days are also presented. The overall distribution shows maxima of outgoing radiation near 20°N. and 20°S. with lower values toward higher latitudes in both hemispheres and in equatorial regions. Comparisons of these measurements from TIROS II with previous estimates of outgoing long-wave radiation by investigators of the heat budget show relatively good agreement.

## PREFACE

One of Dr. Harry Wexler's major interests in meteorology was in the atmospheric heat sources and their relation to the general circulation. In his strong advocacy of meteorological satellites in the mid-1950's he foresaw the possibilities of measuring time variations in the radiative energy supply received by the earth-atmosphere system to see how they were related to changes in the planetary flow patterns over a broad spectrum of time periods ranging from days to many years. He was hopeful that satellite data would reveal connections between heating in equatorial regions and circulation changes in temperate latitudes of both hemispheres and that they would also reveal more about interactions between the circulation regimes in the two hemispheres.

Investigations of these questions with the aid of satellite radiation data are in their very early stages, but already there are signs that some of his hopes may be fulfilled. In the ensuing report of a study of outgoing long-wave radiation measurements, it may be seen that one is now able to demonstrate on a quantitative basis how this radiation varies with the circulation both in space and with time. It is anticipated that additional satellite data will allow for at least some crude estimates of the net radiational heating, and thus will allow us to look into the

more difficult question of how the radiation affects ensuing changes in the circulation and its energetics.

It is clear that we are now on the threshold of many broad-scale investigations of the relationships between the heat budget as measured by satellites and the general circulation. To a great extent the stimulation of research in this area stemmed from Wexler's enthusiastic conviction that meteorological satellite data would provide new answers to some very fundamental questions about the behavior of the circulation of planet Earth.

## 1. INTRODUCTION

In an earlier paper [20] the writers presented a preliminary large-scale analysis of outgoing long-wave radiation measurements made by the TIROS II meteorological satellite. That study was based on daily composite charts of radiation data for the Northern Hemisphere between latitudes 20°N. and 55°N. for a total of 25 days in late November and December 1960. The present study is also based on daily composite charts of TIROS II data, but for the entire latitudinal range of the satellite data from 55°N. to 55°S. The period of study is nearly the same as in the previous more limited study—a total of 26 days between late November 1960 and early January 1961. In this paper the radiation data are shown in more detail

in terms of both daily and time-averaged global charts. Comparisons of radiation data with the planetary-scale circulation and its energetics are still limited to the Northern Hemisphere, but more details of the relationships between the radiation fields and the large-scale circulation are presented.

## 2. DATA USED

The net outgoing long-wave radiation data studied in this paper are derived from measurements by channel 4 of the five-channel radiometer on TIROS II [3]. This channel measures intensity of radiation in the spectral range of approximately 7–33 microns. The measurements are made at differing zenith angles which vary over each scan of the radiometer and over each orbital pass of the satellite. The filter of the channel 4 radiometer has a transmittance which is not invariant with wavelength. All of these characteristics offer limitations which must be overcome to derive the total outgoing radiative flux. Methods of adjusting these data to obtain values of radiative flux from any channel 4 measurement have been developed by Wark et al. [16, 17] and their procedures were applied to the data used in this study. (Admittedly their procedure was a first approximation, particularly in regard to limb-darkening effects, and it is likely that newer corrections based on empirical limb-darkening for TIROS II data would make for somewhat greater accuracy in the flux values, but these have not as yet been applied to these data.)

These adjusted channel 4 data have been examined on a broad scale through use of daily composite radiation charts, each consisting of all radiation data obtained within one day's sequence of orbital passes. These charts were prepared on a Mercator map projection covering the entire latitudinal range of the data (approximately 55°N.–55°S.). The actual observation times for these composites cover a considerable portion of a 24-hr. period as the orbital track shifts westward with time due to the rotation of the earth. At any given latitude (except north of about 40°N. and south of about 40°S.) the measurements are taken very close to either one or two<sup>1</sup> specific local times during a 24-hr. period. At latitudes poleward of 40°N. or 40°S., there may be overlapping of observational scans from several successive orbital passes (as many as four or possibly five orbital passes at locations farthest poleward), so that data are obtained at successive intervals of about 1½ to 2 hours. In all cases where measurements from two or more scans were obtained in a given day for a given grid point<sup>2</sup>, all the data were simply averaged together without regard to observation time.

In addition to being limited to the region between

<sup>1</sup> Two different times if data from both a northbound and southbound orbital pass are received in a day—about 12 hours apart in equatorial regions. Coverage on both north- and southbound passes is restricted to regions in the vicinity of North and Central America because of locations of data-acquisition stations.

<sup>2</sup> Each datum was assigned to the closest grid point in a square array on the Mercator projection. Grid spacing was 2.5° long. In degrees latitude this varies from 2.5° at the equator to about 1.75° at latitude 50°.

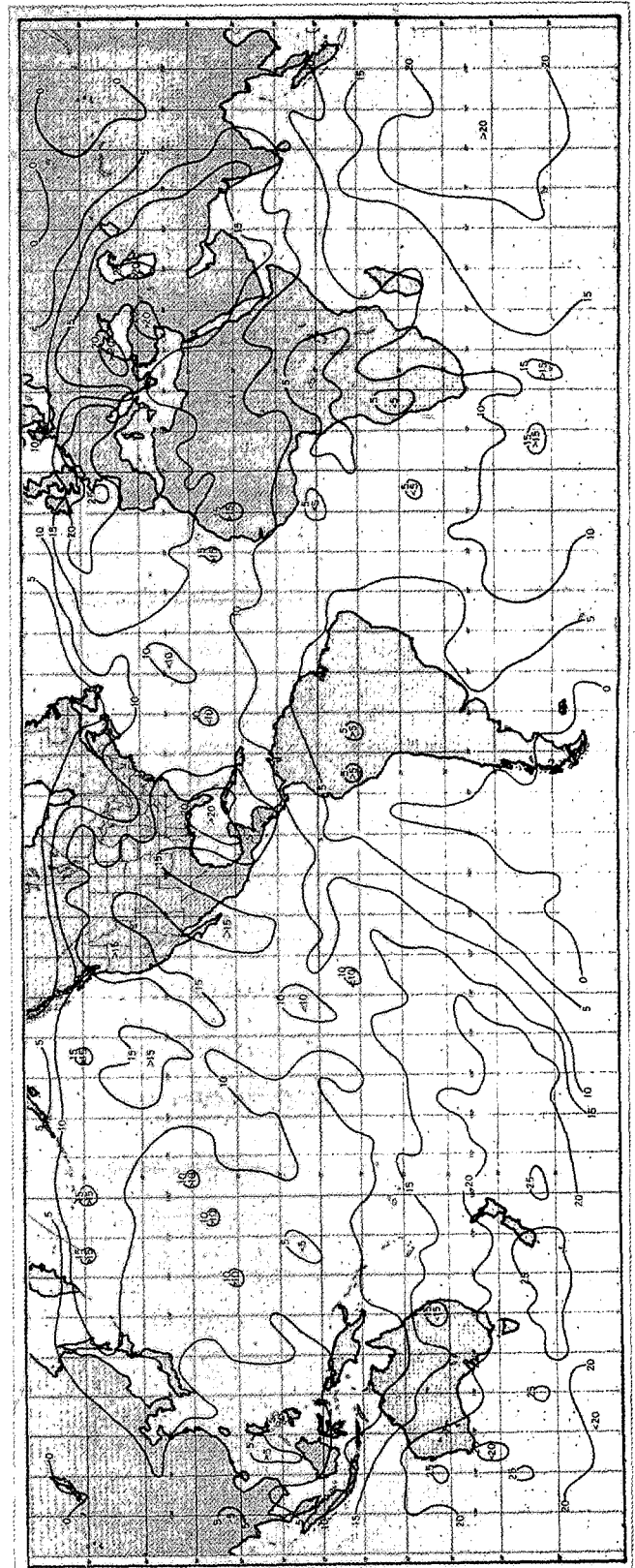


FIGURE 1.—Geographic distribution of number of days in selected period of 26 days in which channel 4 radiation data from TIROS II were available. Isopleths are drawn at intervals of 5 days.

latitudes 55° N. and 55° S. because of the orbit of TIROS II, the global coverage of radiation data was limited by the basic maximum number (8 to 9 per day) of orbital passes that could be interrogated by the two acquisition stations, by technical problems in interrogating on all possible orbital passes or obtaining a sufficiently noise-free signal, and by the elimination of data from two of the three scanning modes of the 5-channel radiometer because of uncertainties of data location.<sup>3</sup>

The TIROS II Users' Manual [15] indicates that the channel 4 radiometer deteriorated after pass 650 (January 6, 1961) and that any data beyond that pass are of doubtful accuracy. Others have raised the possibility of some deterioration in the channel 4 radiometer at an earlier time [19], but this is not definitely established and our analysis of the data does not indicate any definite deterioration before pass 650. From these orbital passes of TIROS II prior to January 6, 1961, we selected those days when there were sufficient data to prepare "global" composite radiation charts. The definition of "sufficient" is of course subjective, but we chose to construct composite radiation charts only on those days when at least three orbital passes of usable radiation data were acquired. This was the case on 26 days between late November 1960 and early January 1961.

Geographically the coverage of radiation data was highly variable during these 26 days due to the nature of the TIROS II orbit and the locations of the two data-acquisition stations. This is shown in figure 1 where it may be seen that in some areas such as the southern Indian Ocean, the South Pacific Ocean, southern Australia, portions of the United States, the eastern Atlantic, Europe, and the Middle East there was rather good coverage, whereas there was very little or no data coverage over South America and vicinity and much of Asia. Also there were relatively few data in equatorial regions (10°N.-10°S.) at most longitudes, largely because of the elimination of data obtained in the "closed mode" which occurred mainly in these latitudes. These large gaps in the data often make it difficult to compare latitudinal or longitudinal distributions of outgoing long-wave radiation from one day to another. However, examination of the data coverage on the 26 daily composite charts showed that there were four periods of 4 or 5 days each, in which all or nearly all of the days had more than the minimum number of orbital passes of data. These four periods were selected for making most of the ensuing broad-scale examinations of the data in both space and time.

### 3. DAILY COMPOSITE RADIATION CHARTS

Samples of daily composite radiation charts for three days of very good data coverage (data from 6-8 orbital passes per day) are shown in figures 2-4. A striking fea-

ture of these charts is the extent of data coverage obtainable from 6-8 orbital passes (out of a potential of 14-15 per day which could be interrogated if additional interrogation facilities and power supply had been available). This coverage, even with the elimination of certain modes of radiation sensor operation as discussed above, is considerably greater than coverage by television pictures. This is so because the television cameras can usually take pictures only over about 15-20 percent of each orbital pass and only during the daylight portion, whereas the radiation data are gathered over nearly the entire orbital pass. Naturally then each composite radiation chart contains data taken both day and night. Figure 5 shows the regions of day-night coverage for the radiation data of figure 2. The day-night zones shift gradually eastward along the orbital passes with time (about 5° long. per day), so there is little difference in the regions of day-night coverage for figures 3 and 4. However, over a period of about 36 days the regions of day and night coverage would be almost completely reversed.

Even though much small-scale detail has already been smoothed out through use of the relatively large grid spacing and in some places through the averaging of data in overlapping orbits, the radiation patterns in figures 2-4 exhibit much detail. For the most part these radiation patterns are related to the fields of cloudiness over the earth, since the overall outgoing infrared radiation is highly correlated with the radiation in the water-vapor window region, and the latter is rather well related to the cloud distributions. Thus low values of radiation are generally associated with well-defined regions of middle or high clouds and high values are representative of regions of low, scattered, or no clouds (cf., [5, 13]).<sup>4</sup>

In view of these relationships it is readily apparent that much widely diversified information about weather systems in many parts of the earth can be deduced from figures 2-4. For instance, it is evident that the inter-tropical convergence zone (or zones) was very active from the central Pacific westward across the Indian Ocean in view of the predominance of low radiation values, whereas it was rather inactive over the eastern Pacific and the Atlantic where radiation values were relatively high.

Over the temperate latitudes of the Northern Hemisphere the areas of low outgoing radiation generally agreed well with the locations of the cloudiness of the cyclones and fronts as found on the synoptic charts (not shown here) while the higher values of outgoing radiation were associated with the cold anticyclones in the westerlies and the subtropical anticyclones to the south of the westerlies. Time continuity of radiation maxima and minima can be followed in figures 2-4 in many parts of the Northern Hemisphere.

In the South Pacific there were several alternating

<sup>3</sup> Only data obtained in the single open mode were used; data acquired in the alternating open or closed modes were excluded (cf., [2]). Fortunately the mode retained was the most dominant of the three modes of operation.

<sup>4</sup> Exceptions to these relationships are of course possible. For example, over snow-covered continental areas, low radiation values may occur with clear skies as well as with high clouds. However, for the predominant portions of the earth covered by radiation data in figures 2-4, the cloud distribution has the strongest influence on the radiation field.

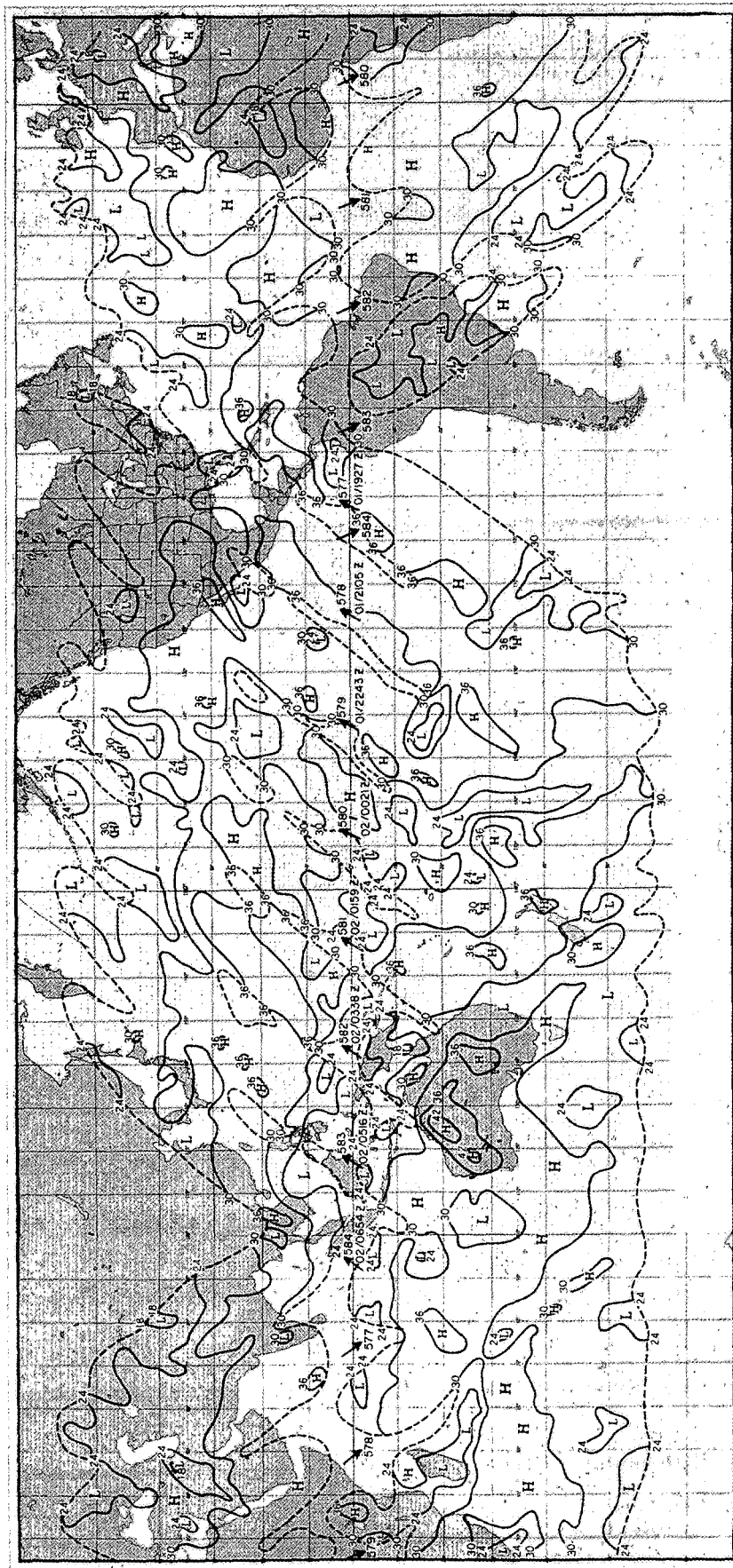


FIGURE 2.—Composite chart of outgoing long-wave radiation for the period January 1, 1961, 1927 GMT to January 2, 1961, 0654 GMT, derived from TIROS II channel 4 data. The units are  $10^{-2}$  ly./min., and the isolines are drawn at intervals of  $6 \times 10^{-2}$  ly./min. H and L refer to maxima and minima of long-wave radiation respectively. The broken lines indicate the boundaries of the data. The arrows indicate the locations at which the orbital paths of the satellite in this period crossed the equator. The number of the orbit and the time (z for GMT) of equatorial crossing (northbound only) are shown near the arrows.

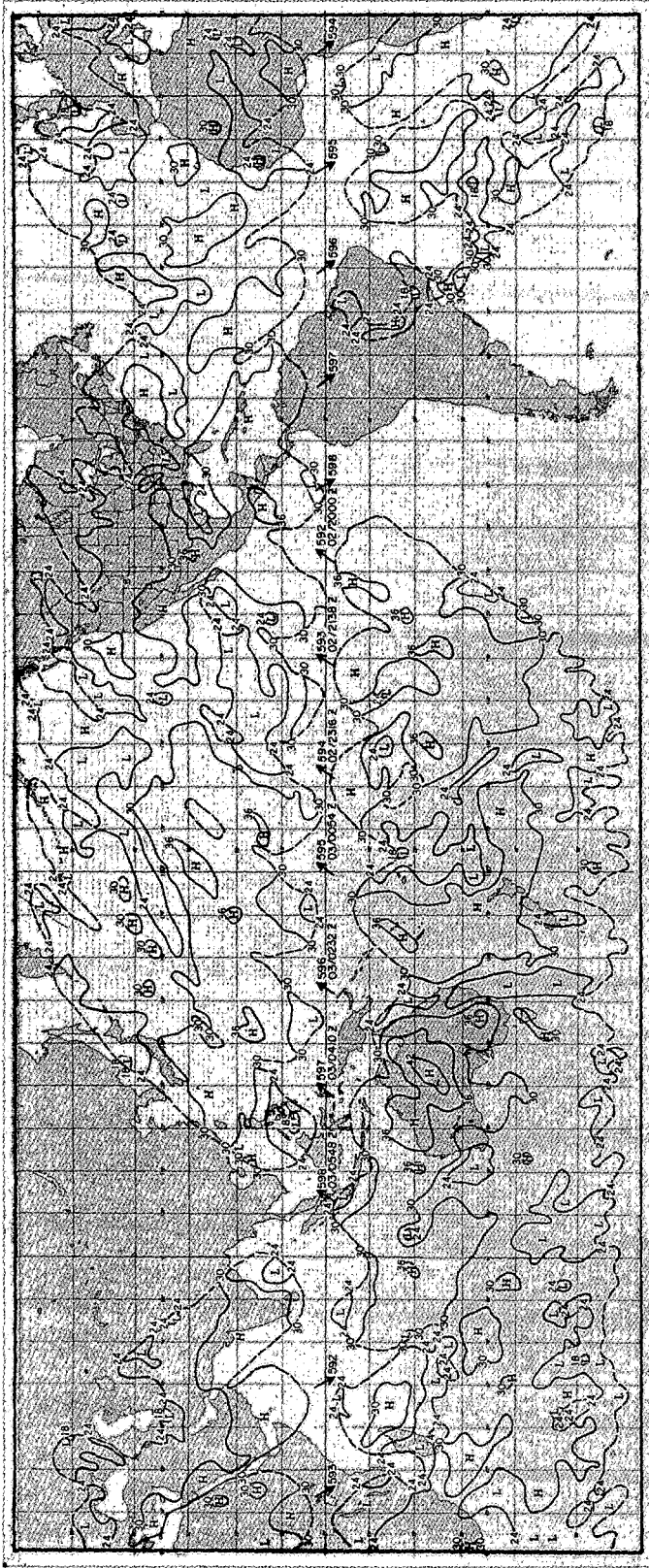


FIGURE 3.—Composite chart of outgoing long-wave radiation for period January 2, 1961, 2000 GMT to January 3, 1961, 0548 GMT. See legend to figure 2.

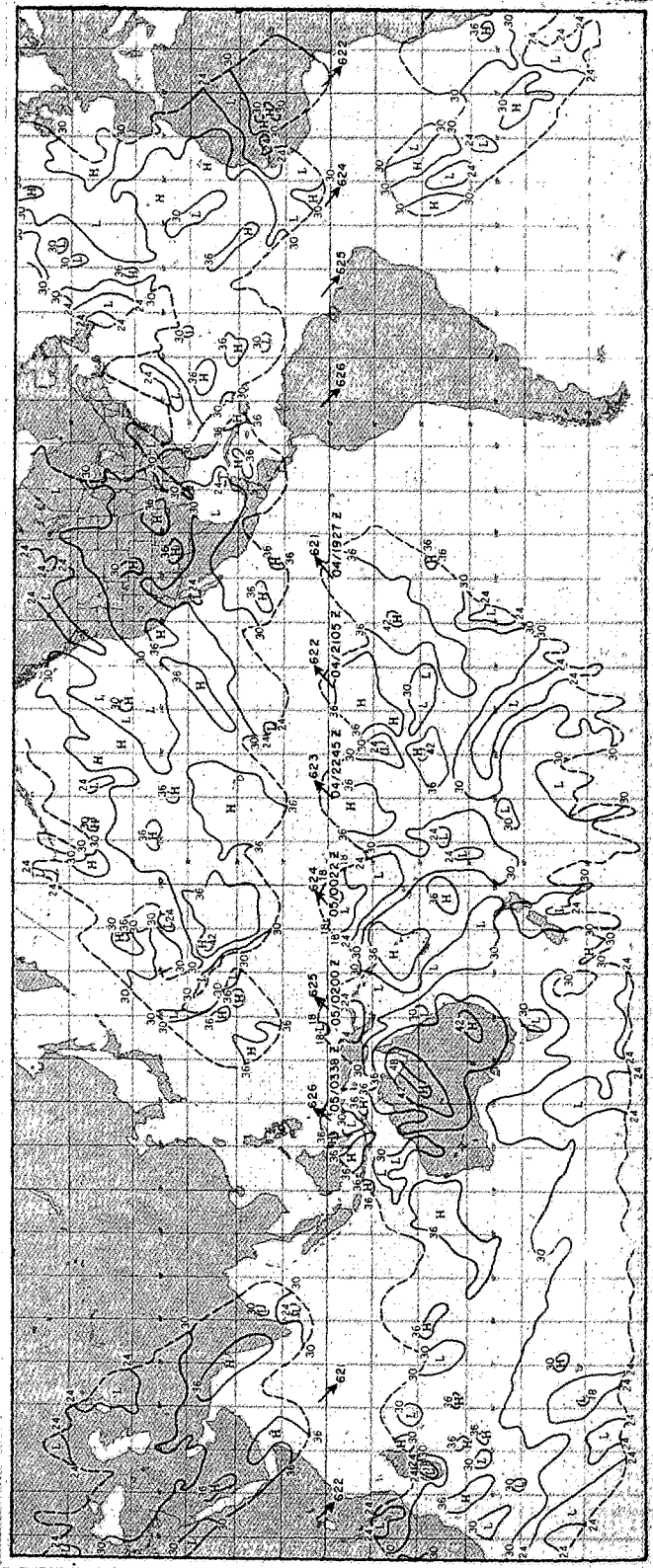


FIGURE 4.—Composite chart of outgoing long-wave radiation for period January 4, 1961, 1927 GMT to January 5, 1961, 0338 GMT. See legend to figure 2.

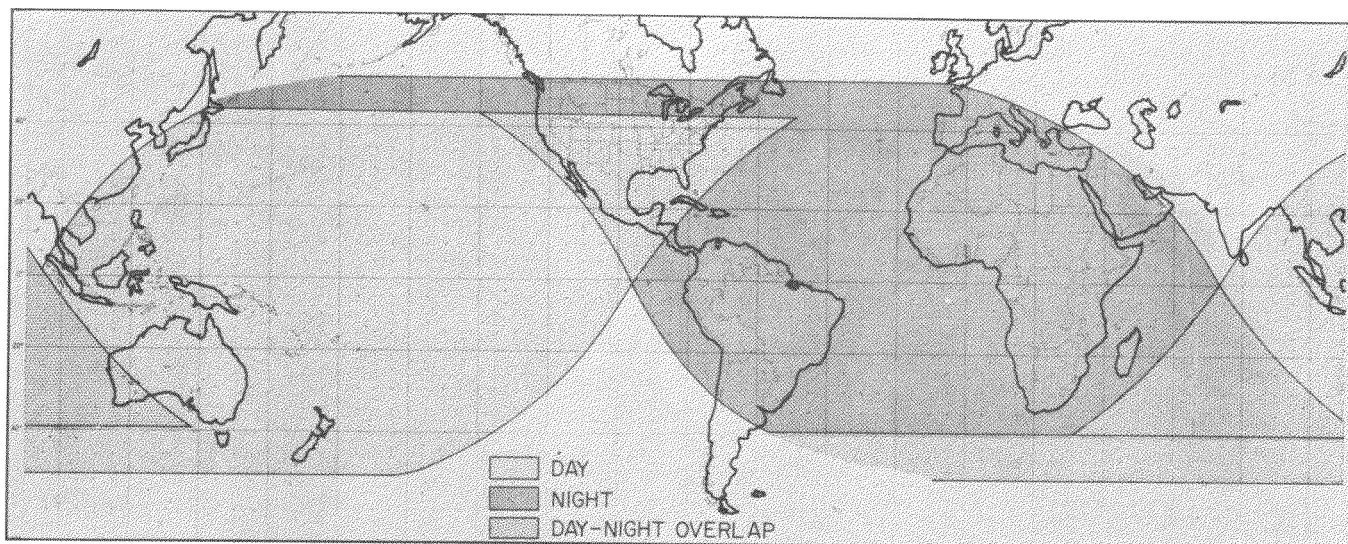


FIGURE 5.—The regions of daytime and nighttime observations and the day-night overlap regions for TIROS II channel 4 radiation data coverage on January 1-2, 1961 (data in fig. 2).

zones of low and high radiation values, basically oriented northwest-southeast between the east coast of Australia and the central Pacific. These zones generally have clearcut continuity in time in the series of maps. Most interesting is the great latitudinal extent of these zones of low and high values of radiation. Indeed it is surprising that in the summer season the convergence and divergence patterns (presumably associated with these radiation fields) were so simply organized over such large latitudinal ranges.

Since these portions of the orbital passes were in daylight (fig. 5) and since the camera viewing angle was satisfactory, there are television pictures of much of this region. Although picture quality on TIROS II was relatively poor, nephanalyses were routinely prepared and a composite nephanalysis for January 1-2, 1961, is shown in figure 6. Comparison of this nephanalysis with figure 2 confirms that the regions of low radiation values were generally associated with large-scale overcast or broken cloudiness and that high radiation values occurred mainly in regions of little cloudiness. The agreement, however, is not perfect and this is generally to be expected. First of all the nephanalyses were those prepared operationally from pictures of poor quality, which makes the nephanalyses less accurate than normal both in interpretation of cloudiness and in precise location of cloud fields. Furthermore, there are bound to be situations when overcast or broken clouds consist mainly of low cloudiness which would result in relatively high radiation values (cf. [5, 13]). This may possibly explain the discrepancy between figures 2 and 6 in such places as east-central Australia and Tasmania, where for example a zone of high values of outgoing radiation, oriented northwest-southeast, was found in a region where considerable cloudiness was analyzed from the pictures.

Much detailed study of the radiation patterns shown in figures 2-4 (as well as the 23 other daily composite radiation charts prepared from TIROS II data) can be made relative to synoptic weather systems; e.g., similar to what was done with Explorer VII data by Weinstein and Suomi [18]. In fact, this can probably be accomplished with more certainty than in their study since the coverage of the TIROS data was generally more comprehensive spatially than the Explorer VII coverage. However, we have proceeded no further with such study of the data, but have rather concentrated on broader-scale study of the radiation data by means of temporal and spatial averaging.

#### 4. TIME-AVERAGED RADIATION CHARTS AND 5-DAY MEAN FLOW PATTERNS

Mean maps of outgoing long-wave radiation for the four periods of good data coverage are shown in figures 7-10. Mean 700-mb. contours and height anomalies for the 5-day periods most nearly coincident with the periods of the radiation data were obtained from the files of the Extended Forecast Branch. These mean 700-mb. data cover only the Northern Hemisphere poleward of about 15° N., and unfortunately no similar hemispheric data were available for the Southern Hemisphere.

Confining our attention first to the portion of the Northern Hemisphere where comparisons with the flow patterns can be made, it may be seen that the fields of outgoing radiation changed markedly between late November (fig. 7) and mid-December (fig. 8), while changes were generally less pronounced during the remainder of December and early January (figs. 9, 10). The most outstanding difference between the radiation fields in figures 7 and 8 was the greatly diminished values of radiation over large portions of both middle latitudes and the subtropics. These changes occurred in association with radical changes

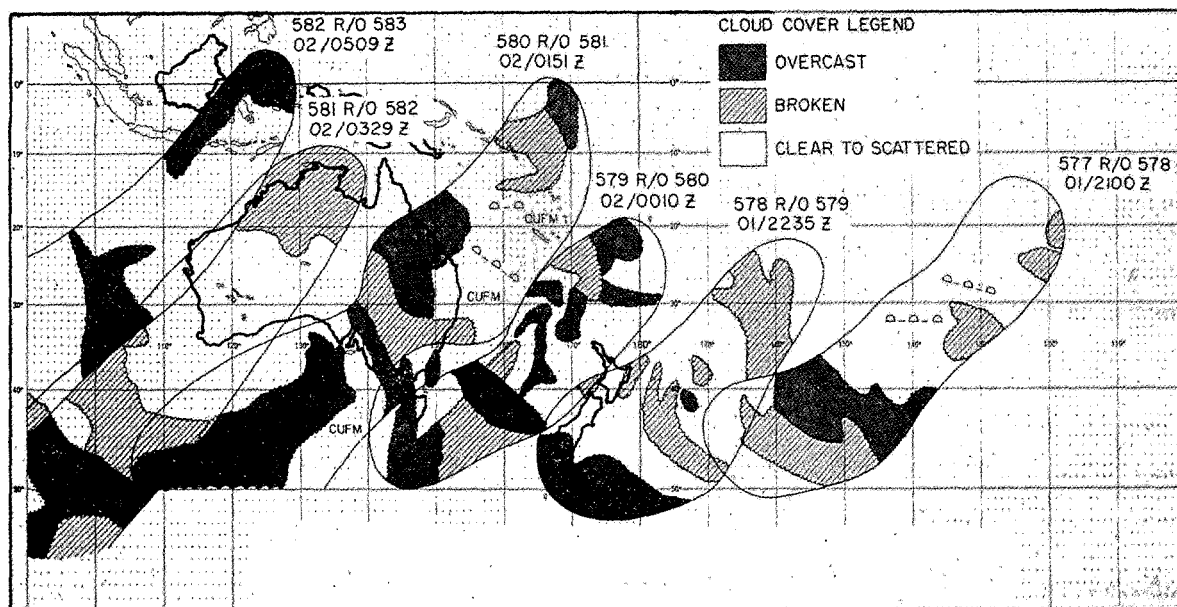


FIGURE 6.—Composite nephanalysis for January 1-2, 1961, prepared from operational nephanalyses based on TIROS II television pictures. The numbers of the actual and the "read-out" (R/O) orbital passes and the date and time (z for GMT) of the pictures are shown for each pass. CUFUM refers to cumuliform cloudiness and lines of cumulus clouds are indicated by a series of standard weather map symbols for fair weather cumulus.

in the 700-mb. mean flow during these periods. From western North America eastward to central Asia the flow shown in figure 7 was basically one of flat westerlies with ill-defined troughs and ridges at middle latitudes and with well-developed zonally-oriented subtropical ridges to the south. The field of height anomalies shows that these westerlies were considerably stronger than normal across the Atlantic and Europe. By mid-December (fig. 8) the flow, from the eastern Pacific eastward into Asia, had changed into a series of large-amplitude, long waves. The height anomalies show that all of these ridges and troughs were stronger than normal. Over the east coast of Asia and the Pacific a large-amplitude wave pattern was in existence in figure 7 and the change was toward a stronger westerly flow in figure 8, but these westerlies were displaced well to the south of normal, as indicated by the strong negative height anomalies over most of the Pacific at middle latitudes. These changes were representative of about the first half of a very large-scale energy, or index, cycle which occurred in the Northern Hemisphere between November 1960 and January 1961. Details of this cycle were treated in terms of energy parameters in our earlier paper [20] and in terms of zonal index in the review of the circulation and weather of December 1960 by Gelhard [6].

Let us return now to our general statement about the diminished values of outgoing radiation between late November and mid-December (figs. 7 and 8). Detailed examination of the radiation data relative to the flow patterns shows that outgoing radiation tended to be considerably lower in those areas where the westerlies penetrated farther southward, i.e., the Pacific (only the cen-

tral and eastern sections can be compared), the eastern United States-western Atlantic, southern Europe and North Africa, and the Middle East. Some relatively high values were still located in these regions, but values below 0.30 ly./min. were more dominant in these zones and there were many more centers of pronounced minima. In most of these regions these centers of low radiation undoubtedly represented centers of major middle and high cloud systems. Over some cold continental regions, such as the United States, however, the lower values may have resulted mainly from more extensive snow cover and lowering air mass and surface temperatures with cold air reaching far southward. In regions where the westerlies shifted northward with time (i.e., the Atlantic and the Near East where ridges developed) radiation values at middle latitudes remained relatively high. This would be expected in association with these stronger-than-normal anticyclonic circulations where pronounced middle and high cloudiness would be suppressed and where warmer air would be advected toward higher latitudes.

Similar relationships between the flow and the radiation patterns hold in figure 9. Only relatively small changes in circulation occurred between figures 8 and 9 and in general the radiation patterns changed little. In the troughs over the United States and North Africa the areas of lower radiation became more extensive. The increase in westerlies across the top of the Atlantic ridge (note the much stronger contour gradient and the southward-shifted positive anomaly center in fig. 9) was accompanied by decreased outgoing radiation between latitudes 40° and 50°N. across the Atlantic, but high values were main-

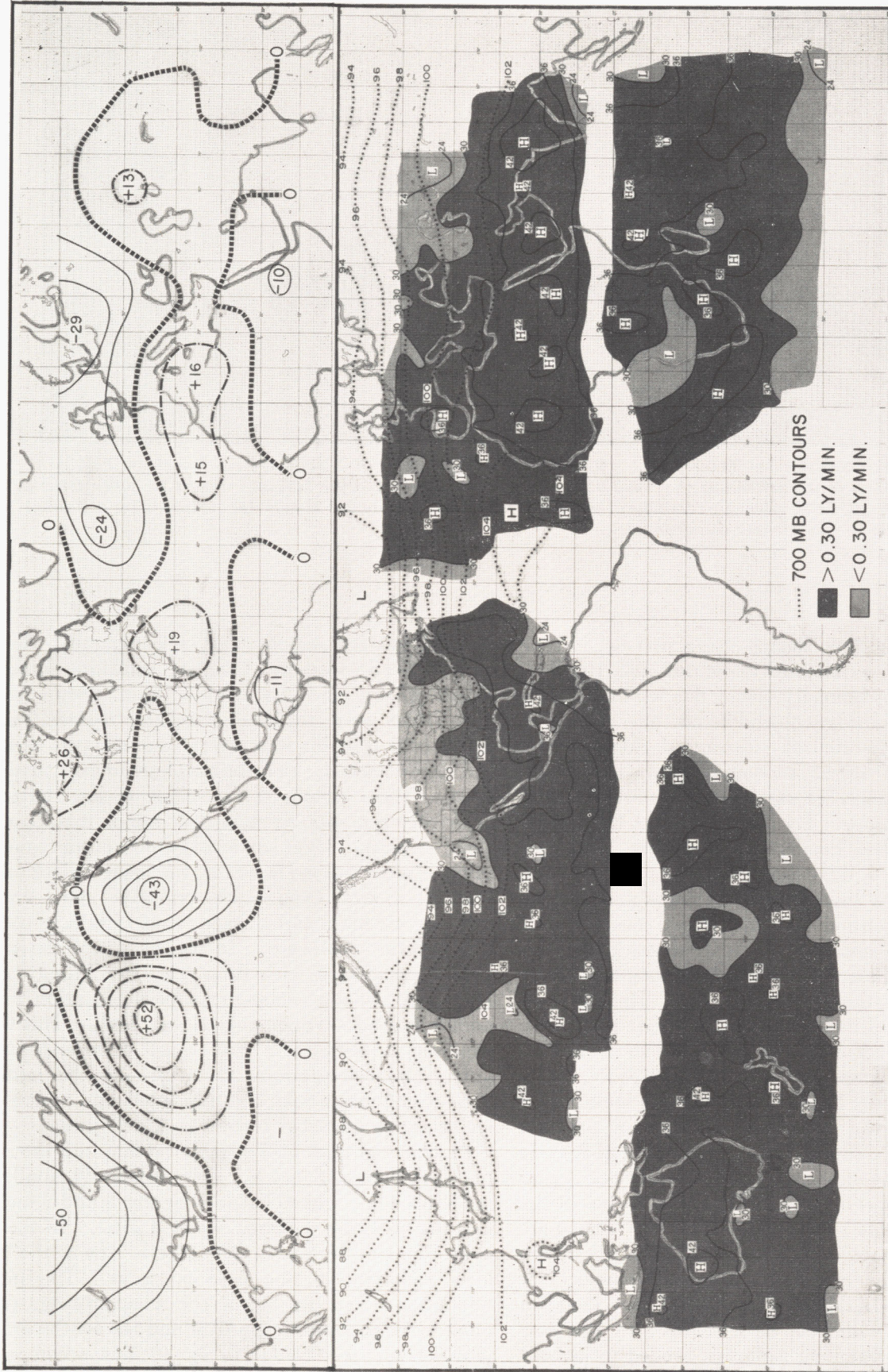


FIGURE 7.—Outgoing long-wave radiation from TIROS II averaged for the period November 26-29, 1960, in lower part of figure. Higher and lower values of radiation are shaded as indicated; unshaded areas are regions of no data coverage. Solid lines are isopleths of radiation labeled in units of  $10^{-2}$  ly./min. and drawn at intervals of  $6 \times 10^{-2}$  ly./min. H and L refer to maxima and minima of radiation, respectively. Superimposed dotted lines in the Northern Hemisphere are 5-day mean 700-mb. contours for the period November 26-30, 1960, at 200-ft. intervals and labeled in 100's of ft. Upper part of figure shows departures from normal of the same 5-day mean 700-mb. height field. Centers are labeled in 10's of feet and isopleths of height anomaly are drawn at 100-ft. intervals. 5-day mean 700-mb. analyses were obtained from the files of the Extended Forecast Branch, U. S. Weather Bureau.

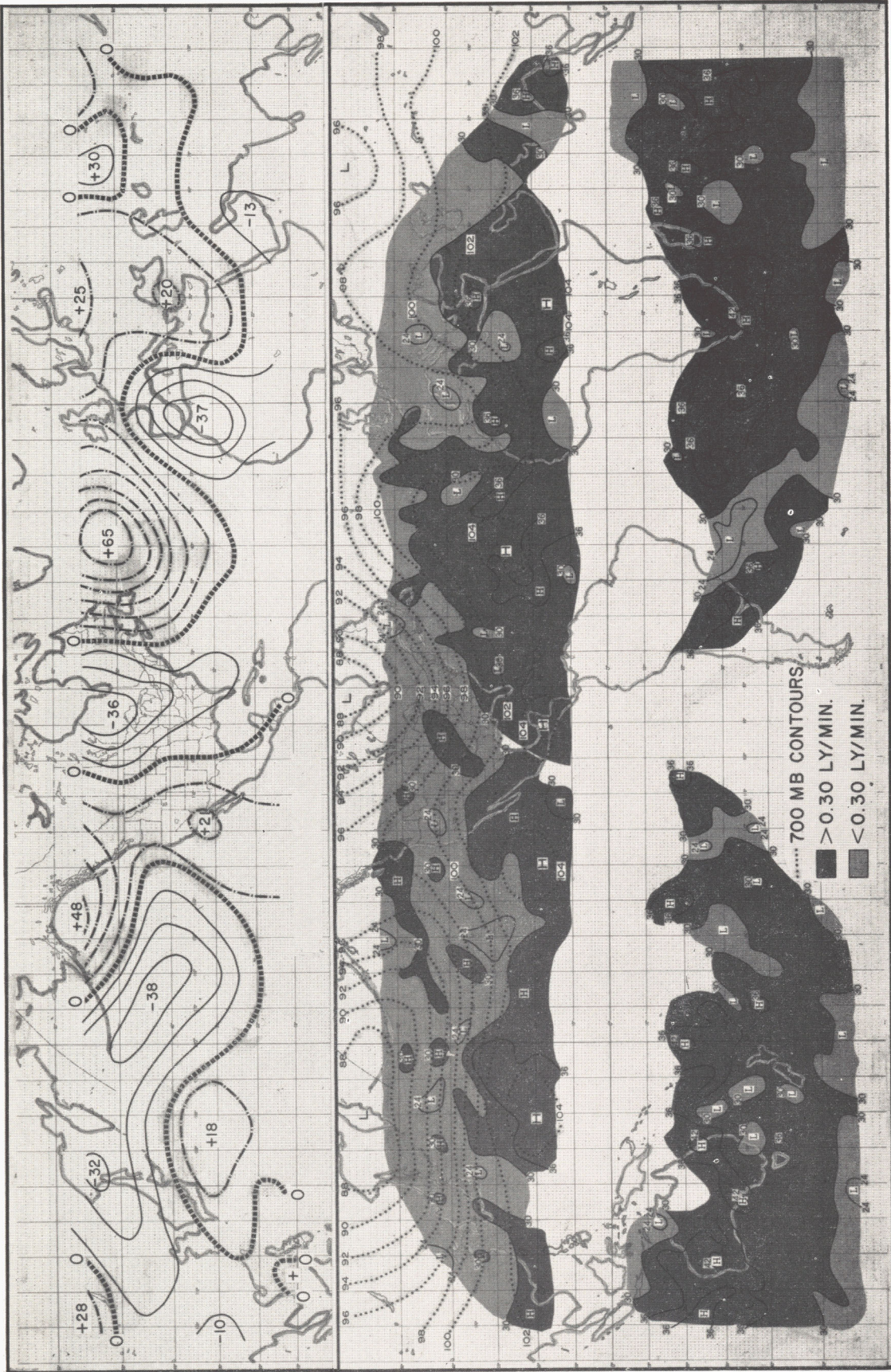


FIGURE 8.—Outgoing long-wave radiation from TIROS II averaged for the period December 14–18, 1960, and 5-day mean 700-mb. height field and departures from normal for the period December 15–19, 1960. See legend to figure 7.

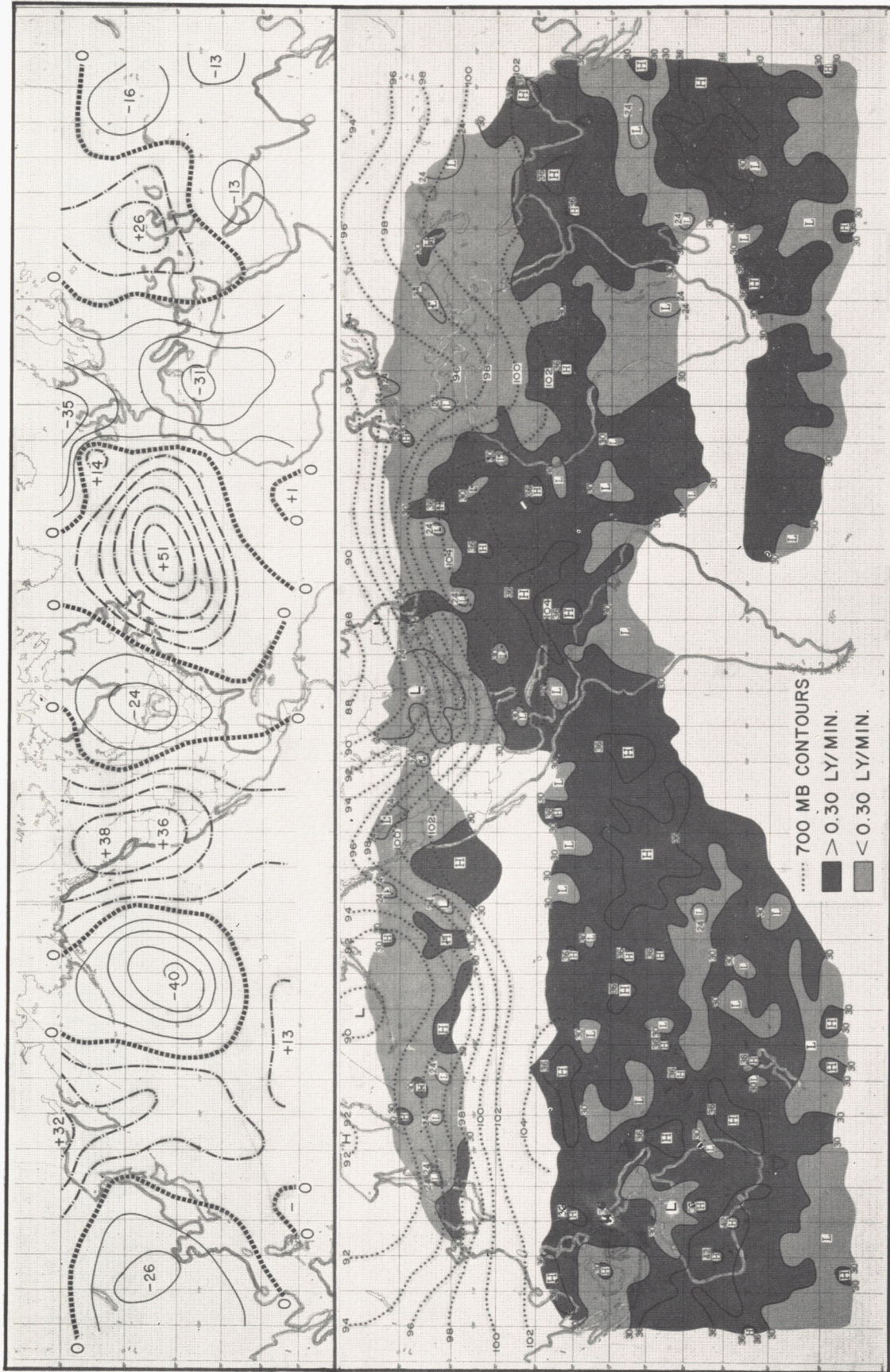


FIGURE 9.—Outgoing long-wave radiation from TIROS II averaged for the period December 21–25, 1960, and 5-day mean 700-mb. height field and departures from normal for the period December 22–26, 1960. See legend to figure 7.

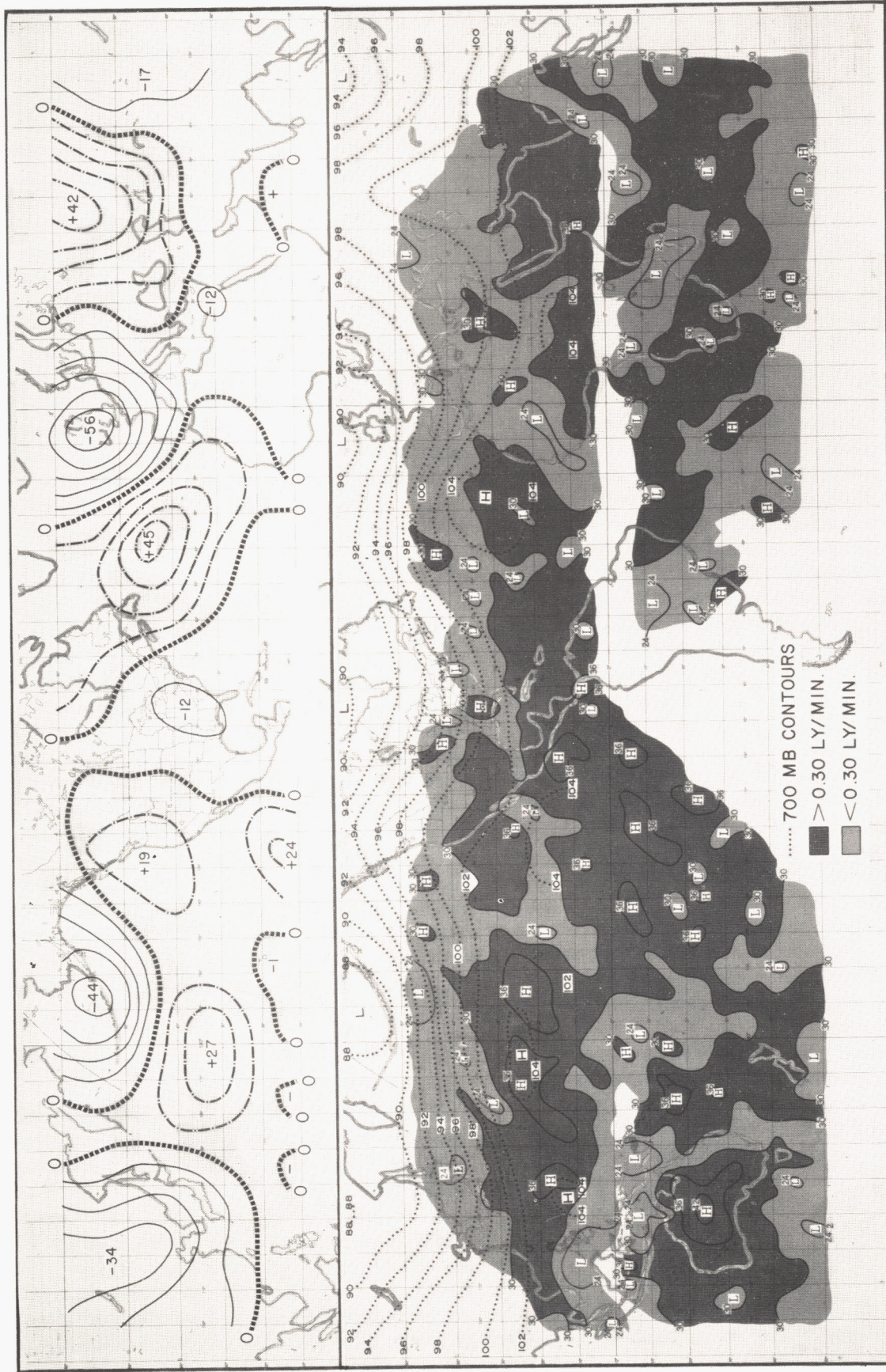


FIGURE 10.—Outgoing long-wave radiation from TIROS II averaged for December 31, 1960, January 2, 3, 4, 1961, and 5-day mean 700-mb. height field and departures from normal for the period December 31, 1960-January 4, 1961. The data for January 4 (see legend to fig. 4) are for nearly 2 days later than the January 3 data (see legend to fig. 3); in all other cases consecutive dates indicate data about 1 day apart. See legend to figure 7.

tained south of the westerlies in the subtropical High. Meanwhile, as the ridge in western North America increased in amplitude, higher radiation values extended northward from the subtropics along the Pacific coast.

In the last period shown (fig. 10), the westerlies had built up again at middle latitudes, particularly over the Pacific and over the Atlantic and Europe, but the flow pattern did not return to the same extreme type of high index regime as in figure 7. Higher values of radiation were becoming more dominant south of the westerlies in the subtropical Pacific (compare figs. 8 and 10—data coverage was lacking in fig. 9), and over the southern United States. However, it is notable that radiation values over the Atlantic north of  $30^{\circ}$  N. were lower than in any other period. With the weakening ridge and increased westerlies, cyclonic and frontal activity originating near the frontal zone along the southeastern coast of the United States was able to penetrate more directly eastward across the Atlantic and hence brought more pronounced zones of middle cloudiness into the Atlantic than previously. Over Europe, North Africa, and the Near East relatively low radiation values still persisted, but the trough over North Africa had broadened out into a longitudinally extensive region of cyclonic curvature.

These comparisons of the time-averaged outgoing long-wave radiation with the time-averaged 700-mb. circulation patterns and their anomalies show that there are some definite broad-scale relationships between them both in space and time. However, it is apparent that the *details* of the mean radiation fields are not so definitely related to the flow. Since to a great extent the radiation field is dominated by the cloud fields, the radiation fields are more dependent on the locations and intensities of cyclones, anticyclones, fronts, and other convergence-divergence areas during the time periods considered. As discussed by Namias [9] these latter elements are generally related to the mean flow pattern, but are also related to such other influences as air mass contrasts, land-sea contrasts, underlying surface temperature and moisture conditions [10], and orographic effects. These influences are not usually reflected explicitly enough in mid-tropospheric flow patterns.

The mean radiation patterns in the Southern Hemisphere did not change as markedly as those in the Northern Hemisphere during the four periods shown in figures 7-10. However, there were signs of changes taking place in a direction somewhat similar to the changes that occurred in the Northern Hemisphere. If the latitudinal zone between about  $20^{\circ}$  S. and  $45^{\circ}$  S. is considered, it may be seen that in late November (fig. 7) the radiation field was dominated by high values which were oriented mainly zonally, particularly from the Indian Ocean eastward into the central Pacific. In mid-December (fig. 8) comparable portions of this latitudinal zone were still basically dominated by zonally-oriented, high radiation values, although some increase in centers of low radiation had occurred.

Later in December (fig. 9) these areas of lower radiation increased just slightly. However, by the last period (fig. 10) the whole pattern was considerably more meridional, with latitudinally extensive regions of low radiation alternating with regions of high values around most of the hemisphere. (Some of these characteristics of the radiation pattern in this period and their relationship to cloudiness were discussed earlier in connection with the daily radiation charts.) This type of change in the radiation patterns from zonal to meridional suggests that the wave pattern in the Southern Hemisphere may have changed from one of relatively high index during late November and much of December to one of relatively low index by early January. Unfortunately we do not have conventional meteorological data on hand at this writing to confirm, even partially, such an estimate. However, in view of the basic relationships found between flow patterns and radiation data in the Northern Hemisphere, it is likely that with more experience in relating these data to circulation one could make some skillful estimates of the state of the large-scale circulation in the Southern Hemisphere.

For the equatorial regions (i.e.,  $10^{\circ}$  N. to  $10^{\circ}$  S.) there were unfortunately large gaps in the radiation data in figures 7 and 8. The coverage was relatively good in the two later periods, however, particularly over the Pacific and Indian Oceans (figs. 9 and 10). Note that in the western Pacific the equatorial area covered by low radiation values increased markedly between these two periods which suggests a major intensification in activity in the intertropical convergence zone. On the other hand, predominantly high radiation values over the eastern half of the equatorial Pacific in both figures 9 and 10 suggest that there was virtually no activity in the intertropical convergence zone in both these periods. Even the limited coverage of data in figure 7 suggests that a similar regime of low or little cloudiness existed in that region in late November. Over the Indian Ocean, Africa, and apparently South America rather extensive zones of low radiation values, and hence extensive cloudiness, existed south of the equator in both figures 9 and 10, while across the Atlantic there appeared to be only a few active zones of low radiation and cloudiness.

##### 5. TEMPORAL VARIATIONS OF LATITUDINALLY-AVERAGED LONG-WAVE RADIATION

Some of the features of the mean radiation charts discussed in the previous section are summarized in figure 11, where latitudinal profiles for the four periods are shown for both the Northern and Southern Hemispheres between latitudes  $20^{\circ}$  and  $50^{\circ}$ . Also shown are corresponding profiles for the zonal kinetic energy in the Northern Hemisphere for the layer 850-500 mb. For the Northern Hemisphere this is similar to figure 3 of [20] except that the data have been grouped into four periods of better data coverage and of more nearly equal length than the three periods used previously. (Astling and Horn [1] have also shown the temporal variations of the

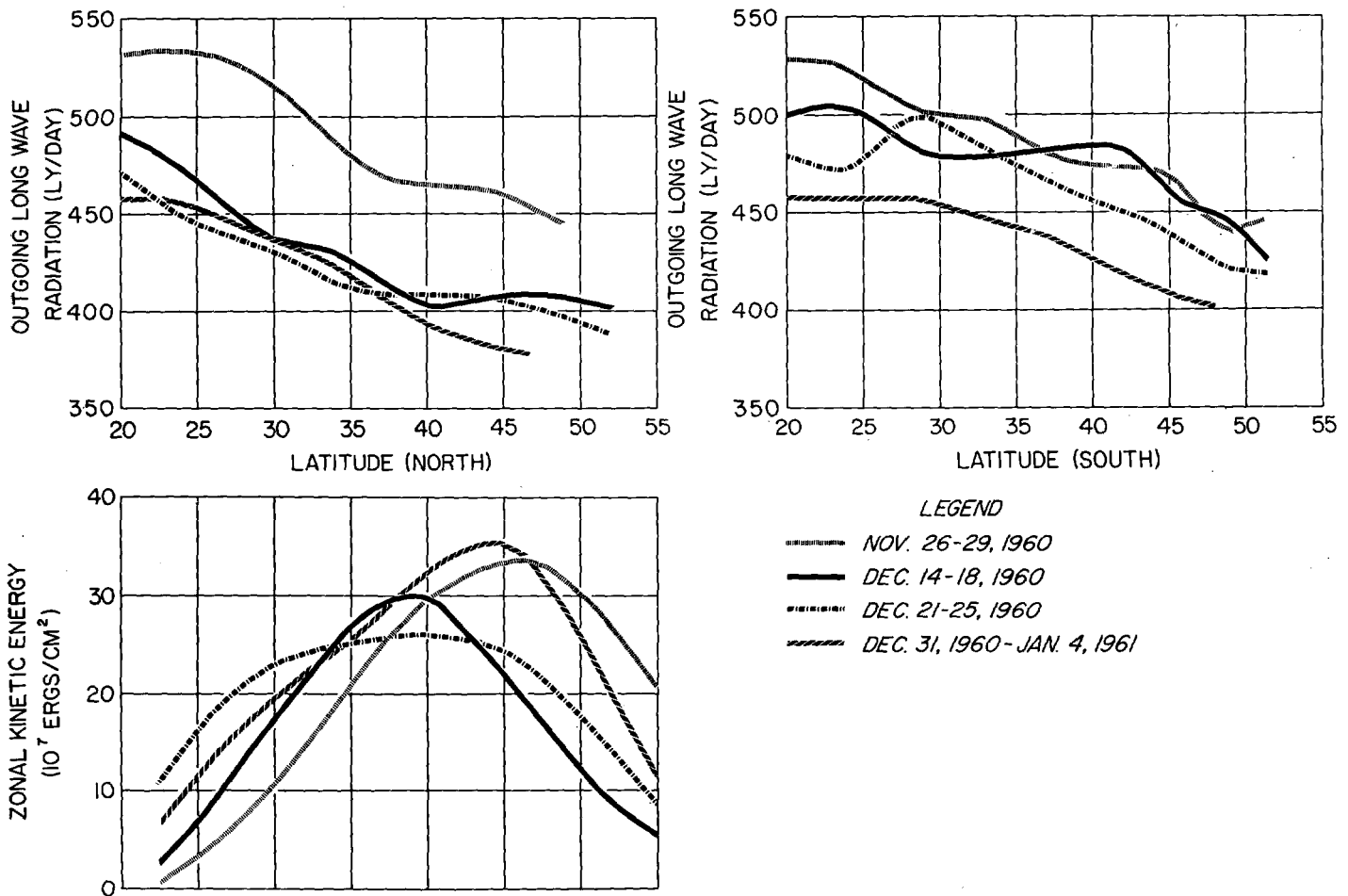


FIGURE 11.—Latitudinal variations of outgoing long-wave radiation from TIROS II for Northern (upper left) and Southern (upper right) Hemispheres and of zonal kinetic energy in the layer 850–500 mb. for the Northern Hemisphere (lower left) for the four periods of good radiation data coverage. Radiation data summarize the fields shown in figures 7–10.

latitudinal average values of these radiation data for a slightly different grouping of mean periods and for all latitudes from 50°N. to 50°S.)

The basic difference between the temporal variations of the latitudinally averaged outgoing radiation in the Northern and Southern Hemispheres is readily apparent in figure 11. In the Northern Hemisphere the largest decline in outgoing radiation at all latitudes occurred between late November and mid-December, whereas in the Southern Hemisphere the greatest drop occurred mainly between mid-December and early January. Also, it is clear that the radiation in the Southern Hemisphere was generally greater and showed less north-south gradient than in the Northern Hemisphere.

In the Northern Hemisphere the association of lower values of radiation in the subtropics (south of about 40° N.) with increased zonal kinetic energy (westerlies) in those latitudes was quite clear, but the changes in radiation north of 40° N. were not especially related to changes in the westerlies. For with a decrease in wester-

lies in these latitudes it might be expected that there would be some net decrease in middle and high cloudiness (while clouds were more extensive farther south). However, whatever tendency there may be in this direction is probably overshadowed in the clear or low cloud areas by the effects of lowering temperatures associated with outbreaks of polar or Arctic air and increased snow cover over continental regions. Some evidence for this is presented in figure 12 where profiles of mean virtual temperature obtained from 850–500-mb. thickness are shown for the various periods. For the whole Northern Hemisphere the temporal changes in thickness were relatively small (lower left, fig. 12), but when only those points where radiation data were available were considered (upper left, fig. 12), the relative variations in the mean temperature profiles in the various periods showed more resemblance to the radiation profiles in figure 11, at least north of about latitude 35° N. This can be seen more readily by comparing the changes in these mean temperatures and in radiation values (in terms of equivalent black body

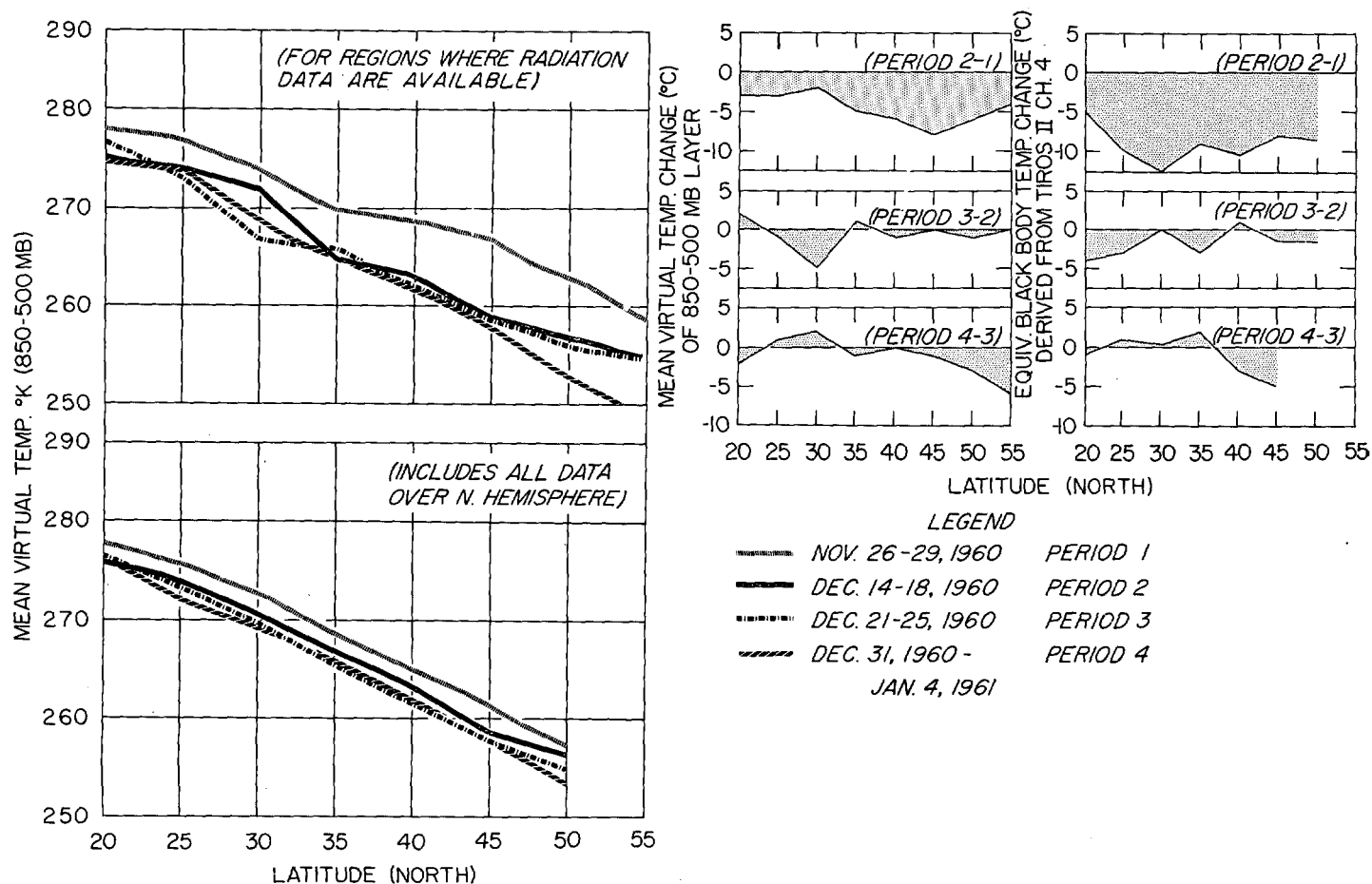


FIGURE 12.—Left side—Latitudinal variation of mean virtual temperature over the Northern Hemisphere for the four periods considered in figures 7–11. Lower graph shows mean temperatures averaged over all longitudes, upper graph shows mean temperatures averaged only at those longitudes where radiation data were available in the particular period. Right side—Latitudinal distribution of changes from one mean period to the next of mean virtual temperature (only for longitudes where radiation data were available) and of equivalent black-body temperatures derived from TIROS II channel 4 data.

temperatures) between the various periods on the right side of figure 12. In general, north of about 35°–40° N. the changes in equivalent radiation temperatures were not very different from the changes in mean temperature in the layer 850–500 mb., which tends to support at least crudely the thesis that lowered air mass temperatures could account for the lowered outgoing radiation at these latitudes. On the other hand, south of 35° N., particularly between periods 1 and 2, the changes in radiation were poorly related to temperature changes. This is as expected since our earlier examination of the flow and radiation patterns definitely suggested that increased middle and high cloudiness were responsible for the decreases in outgoing radiation.

#### 6. COMPARISON OF THE LATITUDINAL DISTRIBUTION OF OUTGOING LONG-WAVE RADIATION DERIVED FROM TIROS II WITH THEORETICAL STUDIES

In our earlier study [20] overall latitudinal average values for outgoing long-wave radiation measured by TIROS II between 20° N. and 55° N. were shown in comparison with theoretical values of Houghton [7], London

[8], Raethjen [12], and Simpson [14]. Figure 13 shows the overall averages of each day's latitudinally averaged radiation for the entire latitudinal range of TIROS II as compared with theoretical estimates by all of the above investigators and also by Baur and Philipps [4]. As was noted for the Northern Hemisphere in [20], the values of outgoing long-wave radiation derived from TIROS II measurements during the 26 selected days of good data are generally in fair agreement in magnitude and latitudinal variation with previous estimates based on theory and empiricism. The closest overall agreement for the Northern Hemisphere is with London's estimate, which is the most recent of those shown. In the Southern Hemisphere the only comparison possible is with Simpson's curve, which is much lower than the curve of TIROS II values, but generally shows some resemblance in latitudinal variation.

The maxima of outgoing radiation in the subtropics near 20°N. and 20°S. are rather clearcut in the TIROS II curve. It is interesting that the maximum in the Southern Hemisphere is slightly greater than the maximum in the Northern Hemisphere, which is contrary to Simp-

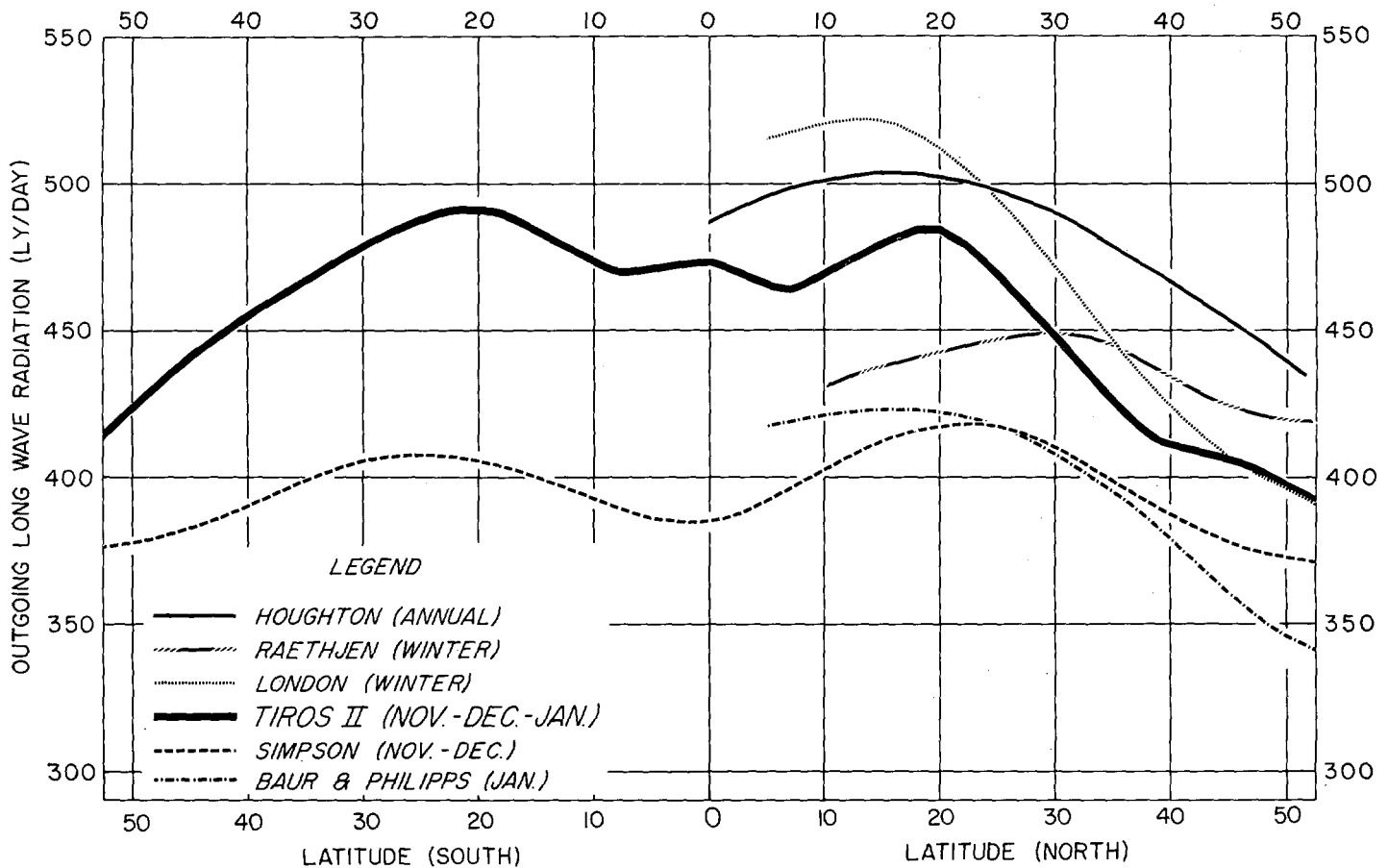


FIGURE 13.—Average latitudinal variation of outgoing long-wave radiation from TIROS II for all 26 days on which composite radiation charts were prepared between late November 1960 and early January 1961, in comparison with estimates made by several investigators of the heat budget.

son's estimate that the maximum in the Southern Hemisphere would be the lower of the two in these months, mainly because of relatively high cloud amounts in the Southern Hemisphere in summer. However, the gradient of radiation between the subtropical maximum and about latitude  $40^\circ$  in the TIROS curve is stronger in the Northern than in the Southern Hemisphere, which tends to agree with Simpson's relative gradients for this time of year. One interesting feature of the TIROS curve, which is not indicated in any of the theoretical studies, is the weak double minima at about  $8^\circ\text{N}$ . and  $8^\circ\text{S}$ . and the weak maximum near the equator. This suggests that on the average for all longitudes there may be two zones of maximum convergence straddling the equator.

Naturally all of these characteristics of the TIROS radiation profile and its comparison with the other curves in figure 13 must be considered highly tentative in view of the relatively small data sample, the highly variable geographical coverage (fig. 1), the variable time of day at which observations were made, and some uncertainty about proper instrument calibration and proper limb-darkening corrections. For example, bias in the sample

of data due to the predominance of low-index type flow in the Northern Hemisphere during the period, as was demonstrated earlier, could mean that the average TIROS II radiation values in the Northern Hemisphere were generally somewhat lower than values representative of a circulation pattern closer to the normal state for this time of year.

It is interesting too that differing methods of selecting, averaging, and/or adjusting the TIROS II measurements for the whole period of record result in some not insignificant differences in latitudinal profiles of outgoing radiation (compare fig. 6 of [1] and fig. 3 of [11] with fig. 13). These differences indicate that there are very likely some uncertainties in the quality and proper physical treatment of the data, but unfortunately they also indicate some differences of opinion concerning the proper statistical procedures for obtaining mean latitudinal values for the period of the TIROS II record.

## 7. CONCLUSION

Despite many uncertainties in the reliability of the TIROS II radiation data and the relatively small and

incomplete global sample of data available, broad-scale examination of the values of outgoing long-wave radiation derived from the TIROS measurements indicates some definitive relations to the planetary flow pattern and its temporal variations. In particular the values of outgoing long-wave radiation in the subtropics and middle latitudes are rather high at the beginning of an energy (or index) cycle; i.e., when north-south thermal gradients are strong (high zonal available potential energy) and the westerlies are and have been strong and relatively flat at middle latitudes (high zonal index). Marked decreases in the outgoing long-wave radiation are found in the low zonal available potential energy (or low index) stage of the cycle, where the westerlies, cold air, and increasing cyclonic activity have penetrated into the subtropics and lower middle latitudes in many places. At the early recovery stage of the cycle (when thermal gradients and westerlies begin to build up in middle latitudes again), the long-wave radiation still remains relatively low, apparently because of cloudiness associated with fronts and cyclones which still persist in association with the previous equatorward displacement of strong thermal gradients.

Variations in long-wave radiation over the Southern Hemisphere were not as great as in the Northern Hemisphere, but a type of variation similar to that in the Northern Hemisphere did occur. The radiation pattern in the subtropics and lower middle latitudes similarly changed from one of zonally-oriented high values to a more meridional type of alternating high and low values, which in view of the associations found in the Northern Hemisphere clearly suggested that the circulation changed from a zonal to a more meridional type (first half of an energy, or index, cycle). Thus it is apparent that satellite radiation data can provide not only direct, comprehensive observations of radiation in the Southern Hemisphere, but also some indirect estimates of the state of the large-scale circulation there.

Over equatorial regions the TIROS data showed variability of outgoing radiation (and hence activity) in the intertropical convergence zone both in space and time. Data were insufficient to show any clearcut relationships to radiation fields and/or flow patterns in parts of the Northern and Southern Hemispheres poleward of about 55° latitude, but the potential for investigating such relationships when more comprehensive data become available in the future is very evident from the planetary-scale radiation fields examined in this study.

#### ACKNOWLEDGMENTS

We thank Mr. W. M. Callicott for providing us with the TIROS II outgoing long-wave radiation data in the form of daily composite charts, and Mr. John Foard, Mr. John Hildebrand, and Mrs. Catherine Frain for assistance in computing the latitudinal average values of radiation.

#### REFERENCES

1. E. G. Astling and L. H. Horn, "A Study of Terrestrial Radiation Measured by TIROS II," *Annual Report* under U.S. Weather Bureau Contract Cwb-10240, Department of Meteorology, University of Wisconsin, Madison, Wis., Sept. 1962, pp. 70-99.
2. W. R. Bandeen, "TIROS II Radiation Data Users' Manual—Supplement," Aeronomy and Meteorology Division, Goddard Space Flight Center, NASA, May 1962, 13 pp.
3. W. R. Bandeen, R. A. Hanel, J. Licht, R. A. Stampfl, and W. G. Stroud, "Infrared and Reflected Solar Radiation Measurements from the TIROS II Meteorological Satellite," *Journal of Geophysical Research*, vol. 66, No. 10, Oct. 1961, pp. 3169-3185.
4. F. Baur and H. Philipps, "Der Wärmehaushalt der Lufthülle der Nordhalbkugel im Januar und Juli zur Zeit der Aquinoktien und Solstitien," *Gerlands Beiträge der Geophysik*, vol. 41, 1934, pp. 160-207 and vol. 45, 1935, pp. 82-132.
5. S. Fritz and J. S. Winston, "Synoptic Use of Radiation Measurements from Satellite TIROS II," *Monthly Weather Review*, vol. 90, No. 1, Jan. 1962, pp. 1-9.
6. R. H. Gelhard, "The Weather and Circulation of December 1960," *Monthly Weather Review*, vol. 89, No. 3, Mar. 1961, pp. 109-114.
7. H. G. Houghton, "On the Annual Heat Balance of the Northern Hemisphere," *Journal of Meteorology*, vol. 11, No. 1, Feb. 1954, pp. 1-9.
8. J. London, "A Study of the Atmospheric Heat Balance," *Final Report*, Contract No. AF19(122)-165, Department of Meteorology and Oceanography, New York University-July 1957, 99 pp.
9. J. Namias, "General Aspects of Extended Range Forecasting," *Compendium of Meteorology*, American Meteorological Society, Boston, 1951, pp. 802-813.
10. J. Namias, "Influences of Abnormal Surface Heat Sources and Sinks on Atmospheric Behavior," *Proceedings of the International Symposium on Numerical Weather Prediction in Tokyo, Nov. 7-13, 1960*, Meteorological Society of Japan, Mar. 1962, pp. 615-627.
11. C. Prabhakara and S. I. Rasool, "Evaluation of TIROS Infrared Data," *Report X644-62-77*, Goddard Space Flight Center, Institute of Space Studies, NASA, Sept. 1962, 27 pp.
12. P. Raethjen, "Wärmehaushalt der Atmosphäre," *Kurzer Abreiss der Meteorologie Dynamisch Gesehen*, vol. 2, Hamburg, 1950, pp. 103-152.
13. P. Krishna Rao and J. S. Winston, "An Investigation of Some Synoptic Capabilities of Atmospheric 'Window' Measurements from Satellite TIROS II," *Journal of Applied Meteorology*, vol. 2, No. 1, Feb. 1963, pp. 12-23.
14. G. C. Simpson, "The Distribution of Terrestrial Radiation," *Memoirs of the Royal Meteorological Society*, vol. 3, No. 23, April 1929, pp. 53-78.
15. Staff Members, Aeronomy and Meteorology Division, Goddard Space Flight Center, NASA, and Meteorological Satellite Laboratory, U.S. Weather Bureau, "TIROS II Radiation Data Users' Manual," Goddard Space Flight Center, Aug. 1961, 57 pp.
16. D. Q. Wark, G. Yamamoto, and J. H. Lienesch, "Infrared Flux and Surface Temperature Determinations from TIROS Radiometer Measurements," *Meteorological Satellite Laboratory Report No. 10*, U.S. Weather Bureau, Aug. 1962, 84 pp.
17. D. Q. Wark, G. Yamamoto, and J. H. Lienesch, "Methods of Estimating Infrared Flux and Surface Temperature from Meteorological Satellites," *Journal of Atmospheric Sciences*, vol. 19, No. 5, Sept. 1962, pp. 369-384.

18. M. Weinstein and V. E. Suomi, "Analysis of Satellite Infrared Radiation Measurements on a Synoptic Scale," *Monthly Weather Review*, vol. 89, No. 11, Nov. 1961, pp. 419-428.
19. R. Wexler, "Synoptic Interpretations and Heat Balance Determination from TIROS II Radiation Data," *Scientific Report No. 1*, Contract No. AF19(628)-429, Aeronautics Laboratories, Concord, Mass., Jan. 1963, 22 pp.
20. J. S. Winston and P. Krishna Rao, "Preliminary Study of Planetary-Scale Outgoing Long-Wave Radiation As Derived from TIROS II Measurements," *Monthly Weather Review*, vol. 90, No. 8, Aug. 1962, pp. 307-310.

## OBITUARIES (continued from p. 481)

- [Obituary on] "Harry Wexler (1911-1962)," by Joanne S. Malkus, *Oceanus*, vol. 9, No. 1, Sept. 1962, p. 24.
- [Obituary on] "Harry Wexler, 1911-1962," *Astronautica Acta*, vol. 8, No. 5, 1962, p. 401.